

Research Article

## Electrical Properties of $(1-x)\text{Ba}(\text{Bi}_{0.5}\text{Ta}_{0.5})\text{O}_3-x\text{BaTiO}_3$ Ceramic System

Jeewan Kumar<sup>†</sup>, S.N. Choudhary<sup>†</sup>, R.N.P. Choudhary<sup>‡</sup> and K. Prasad<sup>†,\*,#</sup>

<sup>†</sup>University Department of Physics, T.M. Bhagalpur University, Bhagalpur 812 007, India

<sup>#</sup>Department of Physics, Institute of Technical and Educational Research, S.O.A. University, Bhubneswar 751 030, Orissa, India

<sup>‡</sup>Aryabhata Centre for Nanoscience and Nanotechnology, Aryabhata Knowledge University, Patna 800 001, India

Accepted 01 March 2016, Available online 05 March 2016, Vol.6, No.2 (April 2016)

### Abstract

Lead-free perovskite  $(1-x)\text{Ba}(\text{Bi}_{0.5}\text{Ta}_{0.5})\text{O}_3-x\text{BaTiO}_3$ ;  $x = 0.25, 0.50, 0.75$  were prepared by conventional ceramic fabrication technique at 1220-1290°C/4h in air atmosphere. X-ray, SEM, electric modulus, dielectric and ac conductivity studies was carried out for characterization. The SEM analysis shows the average grain size to be 0.12 to 0.45  $\mu\text{m}$ . Complex electric modulus analyses suggested the dielectric relaxation to be of non-Debye type. Dielectric studies indicated the relaxor behaviour of  $0.25\text{Ba}(\text{Bi}_{0.5}\text{Ta}_{0.5})\text{O}_3-0.75\text{BaTiO}_3$ . The correlated barrier hopping model was employed to successfully explain the mechanism of charge transport in the system. AC conductivity data indicated the negative temperature coefficient of resistance (NTCR) character of the samples like that of semiconductors.

**Keywords:** Lead free ceramic, Dielectric properties, Relaxor, Electric modulus, AC conductivity.

### 1. Introduction

Oxides with perovskite  $\text{ABO}_3$ -type structure having high dielectric constant play an important role in electronics/microelectronics. Such materials exhibit interesting physical properties and can be potential candidates for multilayer capacitors (MLCCs). The materials used in MLCCs applications are generally all lead bearing compounds. In recent years much attention has been paid to the development of lead free ceramic having either comparable or superior electrical properties than its lead containing counterparts. This is due to the fact that lead containing materials has been restricted for making devices by the EU since Jan. 2004 due to the toxicity of lead oxide, which causes environment pollution during its waste disposal (Prasad *et al.* 2010). The electrical properties of a number of solid-solutions of  $\text{Ba}(\text{Fe}_{1/2}\text{Ta}_{1/2})\text{O}_3$  (Li *et al.* 2004),  $\text{Ba}(\text{Fe}_{1/2}\text{Nb}_{1/2})\text{O}_3$  (Bhagat *et al.* 2014; Yang *et al.* 2012; Singh *et al.* 2012; Intatha *et al.* 2011),  $\text{Ba}(\text{Sm}_{1/2}\text{Nb}_{1/2})\text{O}_3$  (AmarNath and Prasad 2012),  $\text{Ba}(\text{Bi}_{1/2}\text{Ta}_{1/2})\text{O}_3$  (Kumar *et al.* 2014),  $\text{Ba}(\text{Y}_{1/2}\text{Nb}_{1/2})\text{O}_3$  (Prasad *et al.* 2014), with  $\text{BaTiO}_3$  have been reported recently.

An extensive literature survey suggested that no attempt, to the best of authors' knowledge, has so far been made on the lead-free pseudo-binary  $\text{Ba}(\text{Bi}_{0.5}\text{Ta}_{0.5})\text{O}_3-\text{BaTiO}_3$  ceramic system. Both  $\text{BaTiO}_3$  and  $\text{Ba}(\text{Bi}_{0.5}\text{Ta}_{0.5})\text{O}_3$  are described as typical

perovskite-type compounds and could be expected to form a solid solution. Therefore, it is of interest to study the structural and electrical properties of this ceramics. Accordingly, in this report, a new lead-free complex ceramics  $(1-x)\text{Ba}(\text{Bi}_{0.5}\text{Ta}_{0.5})\text{O}_3-x\text{BaTiO}_3$ ;  $x = 0.25, 0.50$  and  $0.75$  [abbreviated hereafter as  $(1-x)\text{BBT}-x\text{BT}$ ] have been synthesized using a high temperature solid state reaction technique and results of their structural, microstructural, electric modulus, dielectric and ac conductivity studies are reported.

### 2. Experimental details

#### 2.1 Preparation of ceramic samples

The polycrystalline samples of  $(1-x)\text{BBT}-x\text{BT}$ ;  $x = 0.25, 0.50$ , and  $0.75$  were prepared by the conventional solid-state reaction technique. High purity (>99.9%) carbonates/oxides of  $\text{BaCO}_3$ ,  $\text{Bi}_2\text{O}_3$ ,  $\text{Ta}_2\text{O}_5$  and  $\text{TiO}_2$  were mixed in proper stoichiometry. Wet mixing was carried out with acetone as the medium for homogeneous mixing. Grinding was performed using mortar pestle for about 2h. Well-mixed powders were then calcined at 1200°C for 4 h under a controlled heating and cooling cycles. The as-calcined powders were compacted into thin circular disk with an applied uniaxial pressure of 650 MPa. The pellets were sintered in air atmosphere at 1220-1290°C in alumina crucible for 4 h. The completion of reaction and the formation of desired compounds were checked by X-ray diffraction technique.

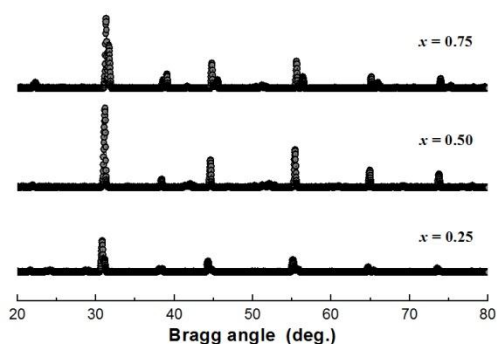
\*Corresponding author: K. Prasad #Also at University Department of Physics, T.M. Bhagalpur University, Bhagalpur 812 007, India

## 2.2 Characterizations

The XRD data were obtained with an X-ray diffractometer (XPERT-PRO, Pan Analytical) at room temperature, using  $\text{CuK}\alpha$  radiation ( $\lambda = 1.5406 \text{ \AA}$ ). The scanning ( $2\theta$ ) was performed from  $20^\circ$  to  $80^\circ$  with a step of  $0.02^\circ$  at a scanning rate of  $1.0^\circ/\text{min}$ . The crystal structures, unit cell dimensions and  $hkl$  values were obtained using Crysfire software. The microstructures of the ceramics have been examined by scanning electron microscopy (SEM) technique. For electrical characterization, pellets were first polished and then electrodes were made using silver paste. The electric modulus, dielectric and ac conductivity data were obtained using a computer-controlled LCR Hi-Tester (HIOKI 3532-50), Japan.

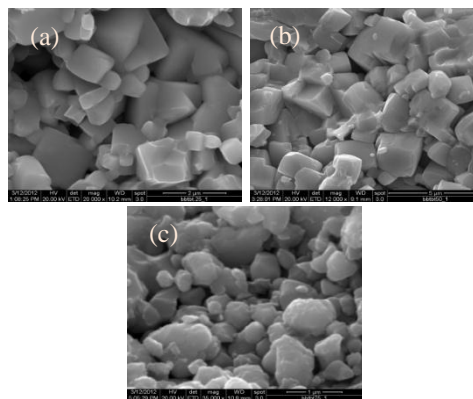
## 3. Results and discussion

Figure 1 illustrates the XRD profiles for BBT-BT ceramic system. Appearance of single and sharp peaks of all the compounds and no other peaks due to any component oxides/carbonates indicated the formation of single phase compounds. The compounds show a single phase orthorhombic structure for all compounds. Therefore, addition of  $\text{BaTiO}_3$  to  $\text{Ba}(\text{Bi}_{0.5}\text{Ta}_{0.5})\text{O}_3$  changes the basic unit cell structure of the solid-solutions. This could be due to the partial replacement of pseudo-cations  $(\text{Bi}_{0.5}^{3+}\text{Ta}_{0.5}^{5+})^{4+}$  with  $\text{Ti}^{4+}$  which produces some kind of disorder in the system and/or due to the difference in unit cell structure of  $\text{Ba}(\text{Bi}_{0.5}\text{Ta}_{0.5})\text{O}_3$  (cubic) (Mishra *et al.* 2012) and  $\text{BaTiO}_3$  (tetragonal). Besides, the difference in the ionic radii of pseudo-cation  $(\text{Bi}_{0.5}^{3+}\text{Ta}_{0.5}^{5+})^{4+}$  and  $\text{Ti}^{4+}$  might have played an important role. Further, shifting in the peak positions and changes in the intensities of peaks could be observed (Figure 1).



**Fig. 1** XRD pattern of  $(1-x)\text{BBT}-x\text{BT}$ ;  $x = 0.25, 0.50$  and  $0.75$  at room temperature

Figure 2 shows the scanning electron micrographs of the fractured surface of BBT-BT ceramics. The photographs contain a very few voids suggesting the high density of the materials. The grains of unequal sizes ( $0.12$  to  $0.45 \mu\text{m}$ ) appear to be distributed throughout the samples. The ratio of the average particle size to the grain size for all the compositions is found to be of the order of  $10^{-3}$ .



**Fig. 2** SEM micrographs of  $(1-x)\text{BBT}-x\text{BT}$  (a)  $x = 0.25$ , (b)  $x = 0.50$  and (c)  $x = 0.75$

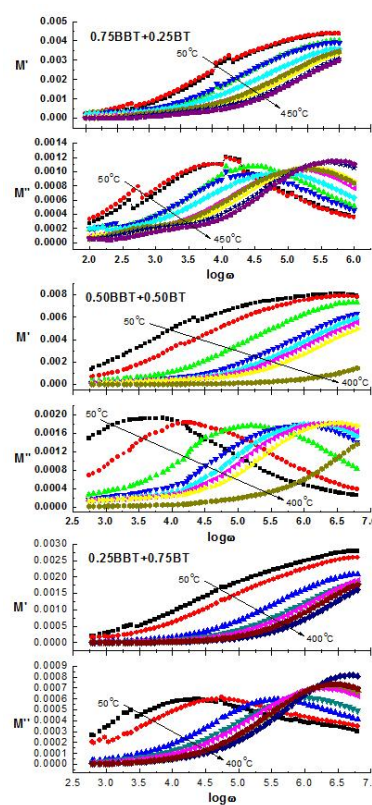


**Fig. 3** Variation of electric modulus of  $(1-x)\text{BBT}-x\text{BT}$ ;  $x = 0.25, 0.50$  and  $0.75$  with frequency at different temperatures

Figure 3 shows the frequency responses of  $M'$  and  $M''$  at different temperatures for  $(1-x)\text{BBT}-x\text{BT}$ ;  $x = 0.25, 0.50$  and  $0.75$ . It is characterized by very low value of  $M'$  in the low frequency region and a sigmoidal increase in the value of  $M'$  with the frequency approaching ultimately to  $M_\infty$ , which may be attributed to the conduction phenomena due to short-range mobility of charge carriers. The variation  $M''$  as a function of frequency is characterized by: (i) clearly resolved peaks in the pattern appearing at unique frequency at different temperatures, (ii) significant asymmetry in the peak with their positions lying in the dispersion region of  $M'$  vs. frequency pattern and (iii)

the peak positions have a tendency to shift toward higher frequency side with the rise in temperature. The low frequency side of the  $M''$  peak represents the range of frequencies in which charge carriers can move over a long distance *i.e.* charge carriers can perform successful hopping from one site to the neighbouring site. The high frequency side of the  $M''$  peak represents the range of frequencies in which the charge carriers are spatially confined to their potential wells and thus could be made localized motion within the well. Therefore, the region where peak occurs is an indicative of the transition from long-range to short-range mobility with increase in frequency. Further, the appearance of peak in modulus spectrum provides a clear indication of conductivity relaxation. Also,  $M''(\omega)$  curves get broadened upon increasing temperature suggesting an increase in non-Debye behaviour. This particular behaviour seems to be unique to electrical relaxation since all other relaxation processes (*e.g.* mechanical, light scattering) typically exhibit opposite behaviour with tendency towards Debye behaviour with increasing temperature.

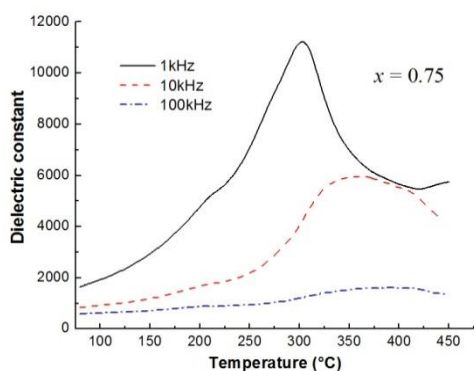


**Fig. 4** Variation of dielectric constant of 0.25BBT-0.75BT with temperature at different frequencies

The temperature dependence of dielectric constant ( $\epsilon$ ) of 0.25BBT-0.75BT at different frequencies is shown in Figure 4. All the plots show a broad ferroelectric to Para electric phase transition (*i.e.* diffuse phase transition, DPT) with strong frequency dispersion, indicating the relaxor behaviour of the compound. It is observed that the phase transition temperature ( $T_m$ ) shifted to higher temperature side (from 305°C at 1kHz to 390°C at 100kHz),  $\epsilon_m$  decreases (from 11237 at 1kHz to 1598 at 100kHz) with the increase in frequency. The above results obtained in BBT-BT, may usher it a possible potential candidate for device applications. A sharp decrease in dielectric constant with the increase in frequency can be explained in terms of the interfacial polarization. Contribution from interfacial polarization comes due to the presence of two layers of materials of different conductivity (Prasad *et al.* 2005).

Figure 5 illustrates the variation of  $\sigma_{ac}$  as a function of frequency at different temperatures for BBT-BT ceramics. It is observed that the patterns of the ac conductivity spectrum show dispersion throughout

the chosen frequency range and with the rise in temperature, the nature of conductivity spectrum appears to be changed.

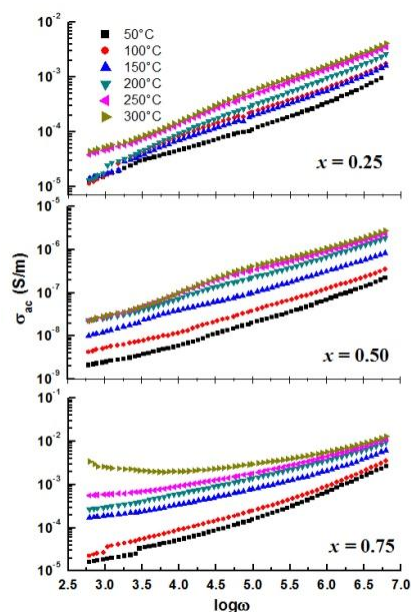


**Fig. 5** Variation of ac conductivity of of  $(1-x)\text{BBT}-x\text{BT}$ ;  $x = 0.25, 0.50$  and  $0.75$  with frequency at different temperatures

The low frequency plateau becomes almost frequency independent at higher temperatures and the frequency dependence of real part of ac conductivity obeys  $\sigma_{ac} = \sigma_o + A\omega^s$ , the Jonscher's power law (Jonscher 1983). The values of the index  $s$  can be obtained from the slopes of the plots ( $\log \sigma_{ac}$  vs.  $\log f$ ). It is observed that the values of  $s$  are always less than 1 and it decreases with the rise of temperature for all the compounds. Besides, the value of  $s \rightarrow 0$  at higher temperatures indicates that the dc conductivity dominates at higher temperatures in the low frequency region and following  $s = 1 + 4/\log(\omega\tau_o)$ . The model based on correlated barrier hopping of electrons predicts a decrease in the value of the index with the increase in temperature. The experimental results follow the same trend. Therefore, the conduction in the system could be considered due to the short-range translational type hopping of charge carriers (Elliott 1978). Also, it is observed that the slope of the curves change with the temperature, which clearly indicates that the conduction process is dependent on both temperature and frequency. The frequency, at which there is a slope change, shifts to higher frequency side upon increasing temperature. The switch from the frequency-independent to the dependent regions show the onset of the conductivity relaxation phenomenon and the translation from long range hopping to the short range ion motion (Mizaras *et al.* 1997). Such dependence is associated with displacement of carriers

which move within the sample by discrete hops of length  $R$  between randomly distributed localized sites. Furthermore, a decrease in the values of  $\sigma_{ac}$  is observed with the rise in temperature for all the compounds, thereby indicating the negative temperature coefficient of resistance (NTCR) character of the samples like that of semiconductors. This may happen due to the accumulation of charge species at the barriers (grain boundaries) which get thermally activated, that plays a dominant role at elevated temperature showing NTCR characteristics.

## Conclusions

Polycrystalline  $(1-x)\text{Ba}(\text{Bi}_{0.5}\text{Ta}_{0.5})\text{O}_3-x\text{BaTiO}_3$ ;  $x = 0.25, 0.50, 0.75$  prepared using a high-temperature solid-state reaction technique, were found to have a perovskite-type orthorhombic structure. Dielectric study of  $0.25\text{Ba}(\text{Bi}_{0.5}\text{Ta}_{0.5})\text{O}_3-0.75\text{BaTiO}_3$  revealed that the compound possess a high dielectric constant of 11237 at 1 kHz, which makes this composition suitable for capacitor application. The ac conductivity study showed the NTCR character of the compounds. The ac conductivity is found to obey the universal power law and the correlated barrier hopping model is found to successfully explain the mechanism of charge transport in the system. These results are well supported by electric modulus data. Complex electric modulus analyses suggested the dielectric relaxation to be of non-Debye type.

## Acknowledgement

The authors acknowledge the financial support provided by the Armament Research and Establishment Board, DRDO New Delhi (Ref. No.: ARMREB/ASE/2008/87).

## References

AmarNath, K., and Prasad, K., (2012), Structural and electric properties of perovskite  $\text{Ba}(\text{Sm}_{1/2}\text{Nb}_{1/2})\text{O}_3-\text{BaTiO}_3$  ceramic, *Adv. Mater. Res.*, 1, 115-128.

- Bhagat, S., AmarNath, K., Chandra, K.P., Singh, R.K., Kulkarni A.R., and Prasad, K., (2014), The Structural, electrical and magnetic properties of perovskite  $(1-x)\text{Ba}(\text{Fe}_{1/2}\text{Nb}_{1/2})\text{O}_3-x\text{BaTiO}_3$  ceramics, *Adv. Mater. Lett.*, 5, 117-121.
- Elliott, S.R., (1978), Temperature dependence of a.c. conductivity of chalcogenide glasses, *Philos. Mag. B*, 37, 553-560.
- Intatha, U., Eitssayeam, S., Pengpat, K., Rujijanagul G., and Tunkasiri, T., (2011), The structural and electrical properties of  $(1-x)\text{BaTiO}_3-x\text{BaFe}_{0.5}\text{Nb}_{0.5}\text{O}_3$  ceramics, *Ferroelectr.*, 415, 176-181.
- Jonscher, A.K., *Dielectric Relaxation in Solids*, Chelsea, New York, (1983).
- Kumar, J., Choudhary, S.N., Prasad K., and Choudhary, R.N.P., (2014), Electrical Properties of  $0.25\text{Ba}(\text{Bi}_{1/2}\text{Ta}_{1/2})\text{O}_3-0.75\text{BaTiO}_3$ , *Adv. Mater. Lett.*, 5, 106-110.
- Li, G., Liu, S., Liao, F., Tian, S., Jing, X., Lin, J., Uesu, Y., Kohn, K., Saitoh, K., Terauchi, M., Di, N., and Cheng, Z., (2004), The structural and electric properties of the perovskite system  $\text{BaTiO}_3-\text{Ba}(\text{Fe}_{1/2}\text{Ta}_{1/2})\text{O}_3$ , *J. Solid State Chem.*, 177, 1695-1703.
- Mishra, A., Choudhary, S.N., Prasad, K., Choudhary R.N.P., and Murthy, V.R.K., (2012), Dielectric relaxation in complex perovskite  $\text{Ba}(\text{Bi}_{1/2}\text{Ta}_{1/2})\text{O}_3$ , *J. Mater. Sci.: Mater. Electron.*, 23, 185-192.
- Mizaras, R., Takashige, M., Banys, J., Kojima, S., Grigas, J., Hamazaki S.-I., and Brilingas, A., (1997), Dielectric relaxation in  $\text{Ba}_2\text{NaNb}_{5(1-x)}\text{Ta}_{5x}\text{O}_{15}$  single crystals, *J. Phys. Soc. Jpn.*, 66, 2881-2885.
- Prasad, K., Chandra, K.P., Bhagat, S., Amarnath, K., Choudhary S.N., and Kulkarni, A.R., (2010), Structural and electrical properties of lead-free perovskite  $\text{Ba}(\text{Al}_{1/2}\text{Nb}_{1/2})\text{O}_3$ , *J. Amer. Ceram. Soc.*, 93, 190-196.
- Prasad, K., Priyanka, AmarNath, K., Chandra K.P., and Kulkarni, A.R., (2014), Dielectric relaxation in  $\text{Ba}(\text{Y}_{1/2}\text{Nb}_{1/2})\text{O}_3-\text{BaTiO}_3$  ceramics, *J. Mater. Sci.: Mater. Electron.*, 25, 4856-4866.
- Prasad, S., Prasad, K., Choudhary, S.N., and Sinha, T.P., (2005), Electrical behaviour of  $0.80\text{Pb}[(\text{Mg,Zn})_{1/3}\text{Ta}_{2/3}]\text{O}_3-0.20\text{PbTiO}_3$  relaxor, *Physica B: Condens. Matter*, 364, 206-212.
- Singh, N.K., Kumar P., and Prakash, C., (2012), Microstructure and dielectric relaxation of BT And ST doped  $\text{Ba}(\text{Fe}_{0.5}\text{Nb}_{0.5})\text{O}_3$  ceramics for sensor applications, *Adv. Mater. Lett.*, 3, 181-187.
- Yang, H., Yang, Y., Lin, Y., Zhu J., and Wang, F., (2012), Preparation and electrical properties of  $(1-x)\text{Ba}(\text{Fe}_{0.5}\text{Nb}_{0.5})\text{O}_3-x\text{BaTiO}_3$  ceramics, *Ceram. Int.*, 38, 1745-1749.